Investigations inside a vaned diffuser of a centrifugal pump at low flowrates.

Investigations inside a vaned diffuser of a centrifugal pump at low flowrates.

A C Bayeul-Lainé[1], P Dupont[2], A Dazin[1], G Bois[1],

[1]LML, UMR CNRS 8107, Arts et Métiers PARISTECH, 8 Boulevard Louis XIV 59000 LILLE

[2]LML, UMR CNRS 8107 Ecole Centrale de Lille Boulevard Paul Langevin, Cité scientifique- CS 20048, 59651 Villeneuve d'Ascq cedex, France

annie-claude.bayeul-laine@ensam.eu

Abstract. This paper focuses on the unsteady flow behaviour inside the vaned diffuser of a radial flow pump model, operating at partial flowrates ($0.387Q_i$, $0.584Q_i$ and $0.766Q_i$ where Q_i is the impeller design flowrate).The effects of the leakage flows are taken into account in the analysis. PIV measurements have been performed at different hub to shroud planes inside one diffuser channel passage for a given speed of rotation, for several flowrates and different angular impeller positions. The performances and the static pressure rise of the diffuser were also measured using a three-holes probe in the same experimental conditions. The unsteady numerical simulations were carried out with Star CCM+ 10.02 code with and without leakage flow. The PIV measurements showed a high unsteadiness at very low flowrate which was confirmed by the numerical calculations. In previous studies it has been shown that the global performances, as the efficiencies are in good agreement between calculations and measurements. In this paper, a joint analysis of measurements and numerical calculations is proposed to improve the understanding of the flow behaviour in a vaned diffuser.

1. Introduction

The purpose of the diffusers of centrifugal pumps is to convert the kinetic energy into static pressure by allowing a more gradual expansion and less turbulent area for the liquid to reduce in velocity. The radial diffuser can be classified into two parts: i-vaneless diffusers, ii-vaned diffusers. The present study will deal with a vaned diffuser. Vaned diffusers are designed for a given flowrate, and so far away from this design flowrates the efficiency of the diffuser and of the pump can become critical. The vaned diffuser has eight diffusing passages wherein the width of the diffusing passage is constant which let us assume that the static pressure is constant along the axial direction. The cross-sectional area of the diffusing passage increases from the inlet radius of the diffusing passage to the outlet radius of the diffusing passage.

Experimental correlations have been widely used in order to design optimum channel diffuser passage geometries assuming steady and uniform inlet flow conditions as proposed by Runstadler [1] and Japikse [2].

For real pump configuration, overall diffuser performances must be analyzed taking into account real inlet flow conditions including inlet angle distribution, blockage effects and leakages, more generally unsteadiness.

Previous experimental results (Wuibaut [3,4]) and numerical ones (Cavazzini [5 to 7]) concerning the pump model used for the present study, have shown that the jet and the wake structure was an unsteady one as expected. Because of the leading edge shape of the vaned diffuser combined with the rather small value of the vaneless radius ratio (R_3/R_2=1.068) of the pump model, non-uniform flow structures are quite present and strong as shown by Si et al. [8]. A deeper analysis from Bayeul-Lainé et al [9-11] and from Dupont et al [12] has also shown that unusual leakage effects occur in the present experimental model, the effects of which may also affect the diffuser performances.

Up to now, diffuser performances have been analyzed for high flowrate values because leakage effects have been considered as negligible. Only velocity fields inside the diffuser have been compared with numerical results up to know. However, for low flowrates, leakage effects cannot be neglected. So more complete comparison studies are performed between experimental and numerical results including pressure evolution and pump model overall performances. This is the reason why this paper presents velocity distribution inside the diffuser channel combined with static pressure evolution inside the diffuser for three flowrates below the nominal one, with more focus on the leakage effects that are quite uncommon in this kind of pump laboratory model.

2. Experimentation

2.1. Test and apparatus

Table 1. Pump characteristics

Impeller		**Diffuser**	
Inlet radius	R_1 = 0.14113 m	Inlet shroud radius	$R_{3'}$ = 0.258 m
Outlet blade radius	R_2 = 0.2566 m	blade leading edge radius	R_3 = 0.2736 m
Outlet shroud radius	$R_{2'}$ = 0.257 m	blade trailing edge radius	R_4 = 0.3978 m
Number of blades	Z_i= 7	Number of vanes	Z_d= 8
Outlet height	B_2 = 0.0384 m	Height	B = 0.04 m
Impeller design flowrate	Q_i = 0.337m^3/s	Diffuser design flowrate	Q_d= 0.8Q_i
Rotational speed	N = 1710 rpm		

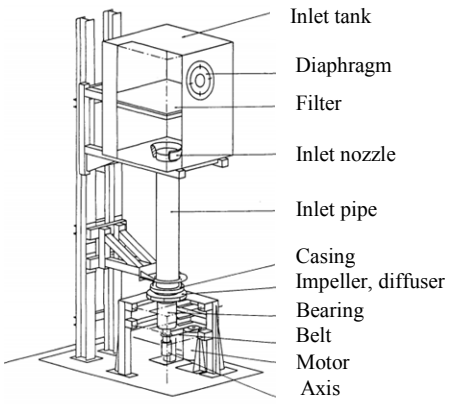

Figure 1. test rig (Morel [13])

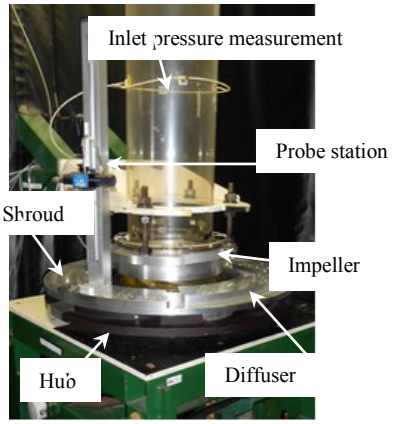

Figure 2. Apparatus: three-hole probe.

The test model corresponds to the SHF pump, working with air, in similarity conditions (Reynolds number) compared to water, for which several studies have been made (Cavazzini et al [5-6]) involving numerical and PIV comparisons. The apparatus rig can be shown in Figure 1.The existing database has been completed by pressure probe measurements for a complete performance analysis in the vane diffuser part of the pump model. The test ring used for the three-hole probe (Figure 2) was the same as the one already developed for the PIV measurement already described in the previous papers, especially in reference [5]. Test pump model and PIV measurements conditions have been already described in several papers [3-7] and main pump characteristics are given in Table 1.

2.2. PIV measurements

PIV measurements have been performed at different hub to shroud planes inside one diffuser channel passage for a given speed of rotation of 1710 rpm and various flowrates. PIV snapshots were simultaneously taken by two cameras positioned side by side and two single exposure frames were taken by each camera every two complete revolutions of the impeller. For each operating condition, the PIV measurements have been trigged with different angular impeller positions (Figure 3). For each angular position, four hundred instantaneous velocities charts have been obtained, covering the space between inlet and outlet diffuser throats. This makes a rather good evaluation of phase averaged velocity charts possible. The PIV results are extracted from the thesis of Cavazzini [2]. In order to do comparisons with the other methods, for each probe position (see paragraph 2.3), mean values of radial, tangential and absolute velocity angle α relative to radial direction inside the diffuser were calculated for the amount of the four hundred instantaneous and of the seven each angular positions.

2.3. Three-holes probe

A directional three holes probe has been used to make hub to shroud traverses [15]. Using a specific calibration one can get total pressure, static pressure, absolute velocity and its two components in radial and tangential direction.

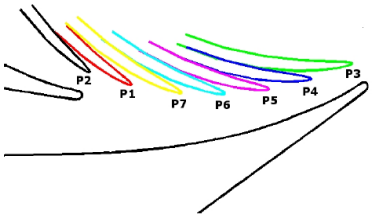

Figure 3. Impeller different angular positions relative to the diffuser vanes

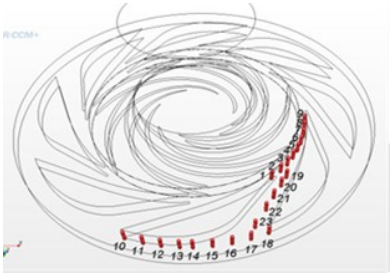

Figure 4. Diffuser measurement locations for probe traverse (10 positions) and unsteady calculations (12 positions).

Figure 5. Sketch of the three-holes pressure probe

In order to well represent the flow field, twenty-three probe locations are defined as it can be seen in Figure 4. For each location, ten axial positions are registered (b*=0.125, 0.2, 0.25, 0.375, 0.5, 0.625, 0.75, 0.875, 0.925, 0.975 from hub to shroud). The probe (Figure 5) is entering inside the diffuser on the shroud side. So it is possible to make measurement close to the wall on the shroud side (b*=0.975), but not on the hub side because of the probe geometry (b*=0.125). The present analysis focuses only on locations 19 to 23 along the blade to blade diffuser channel.

3. Calculations

The numerical simulations were realized with Star CCM+ 10.02 code (RANS frozen rotor and URANS unsteady calculations). Due to the specific model set-up, the effects of fluid leakage gap between the rotating and fixed part of the pump model are unusual and have been analysed and discussed (Bayeul-Lainé et al [10]). Two sources of fluid leakage occur: i-the first one at the impeller inlet (leakage 1, Figure 6, axial clearance = 1mm), ii-the second one between the impeller outlet and the diffuser inlet both for the hub and the shroud sides (leakages 2 and 3, Figure 6, radial clearance = 1mm). To simulate fluid leakage rates, a complete meshing has been set up including the real geometry of the gaps and external domain far upstream the labyrinth. In this respect, boundary conditions include the rotating and the fixed parts of the model casings (Figure 6).

The calculation domain is divided into four domains as can be seen in Figure 6: inlet domain (blue), impeller domain (grey), diffuser domain (braun), outside domain (green).

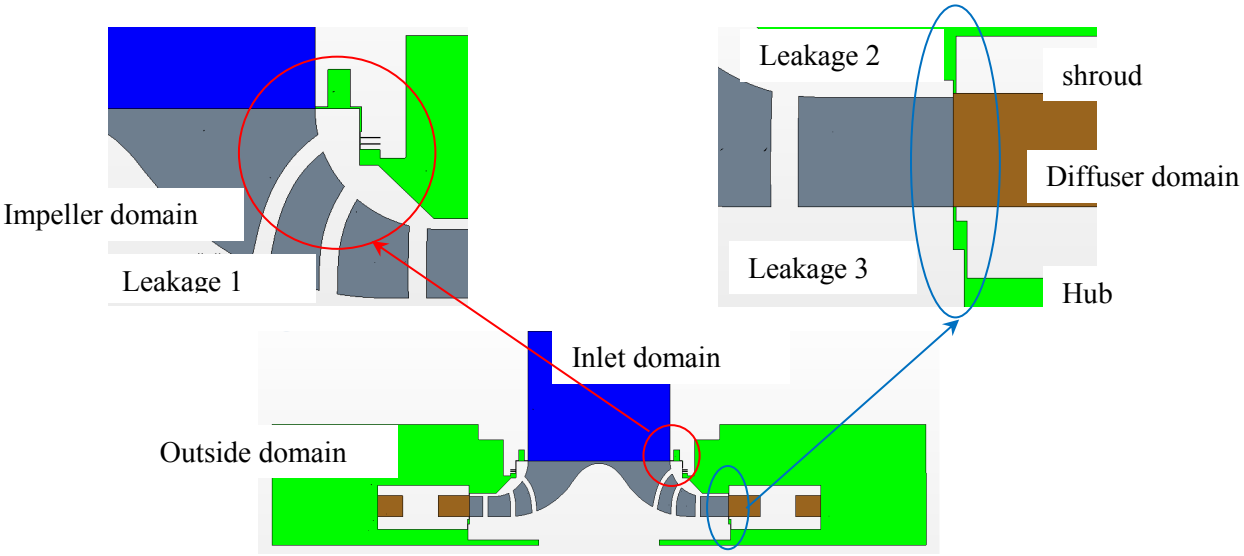

Figure 6. Cut planes of regions modelled: details of fluid leakages' positions.

As thickness gaps are very small (1 mm), a thin meshing model has been chosen. A thin meshing model allows thin regions in the geometry to have a prismatic type volume mesh. Using this kind of mesh improves the overall cell quality and reduces the cell amount when compared to an equivalent polyhedral type core mesh. The number of layers in the thin mesh has been set to 10. In the other parts of the domain, a polyhedral mesh with prism layers is used for all calculations (5 prism layers for a total prism layer thickness of 1 mm). The target size is 3 mm and the minimum size 0.5 mm . The size of the grid is about 20 millions of cells for all the four domains. Concerning the model "without leakages", only Inlet, Impeller and diffuser domains are taken account. The final grid is about 10 millions of cells with the same parameters (base size, surface size, number and size of prism layers). The calculations were done on a tower workstation with Intel-Xeon processor, 12 cores and 64 Go RAM. The CPU time is about 3.10^7 s for the mesh of 10 million of cells and 7 rotations of impeller. Three-dimensional incompressible Reynolds averaged Navier–Stokes equations are solved in steady (frozen rotor) and unsteady states. The SST k-ω turbulence model is used ([Bayeul-Lainé et al. [9], Menter [14]).

The boundary condition at the inlet consisted of a mass flowrate (Q_1*=0.386; 0.584; 0.766). The boundary condition at the outlet was the atmospheric pressure (relative pressure=0 Pa). The boundaries of the outer casing of the impeller are considered as rotating walls. The fluid (air) was considered incompressible at a constant temperature of 20ºC.

For unsteady calculations, the positions of the numerical probe are plotted in the blade to blade channel of the diffuser as can be seen in Figure 4. On the contrary of the physical measurements, the domain of calculations isn't limited by the size of the probe, so two different positions are also taken account (b*=0.025 and b*=0.075, near the hub side) for all positions of the probe.

The convergence criteria are less than 1.e-4. The values of y+ are below 15 in the whole computational domain. The influence of the size of mesh was already tested [11].

4. Results

Before analyzing the fluid inside the vaned diffuser, it is necessary to check that numerical results are in good agreement with experimental ones. The PIV and the numerical methods are non-intrusive ones so they don't modify the flow fluid. But the PIV method can't give the values of pressure and total pressure. The three-holes probe can give this information but this method disturbs the flow fluid. The presence of the probe inside the channel (Figure 7) represents more than 5% of the width of the diffuser throat of the channel (2mm compared to 38,9 mm) and from 3,5 % to 100 % of the locally

depth of the channel. The numerical method is a good compromise to analyze the evolution of the flow fluid if good agreement between all the methods can be checked.

The agreement's checking is done at three different stages:

- By comparison with global performances (static head pump, efficiencies)
- By comparison with quasi-local performances along the diffuser's radius (static head, radial velocity, flow angle inside the diffuser).
- By comparison with local performances in different cut planes (same parameters).

The numerical results are registered at each time step which is equivalent to one degree of rotation for the 23*12 numerical probe's positions. Furthermore, contours of pressure, velocity or flow angle are registered at each time step.

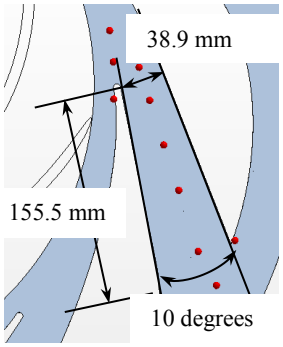

Figure 7. Probe's location

4.1. Global results

These results are given for flowrates between Q_1*=0.386 to Q_1*=1.13, even if the present paper focuses on the three lower flowrates. The numerical model takes into account the fluid leakages.

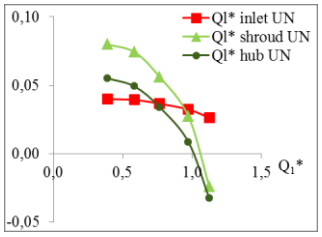

Figure 8. fluid leakages

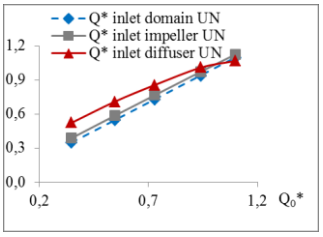

Figure 9. Flowrates

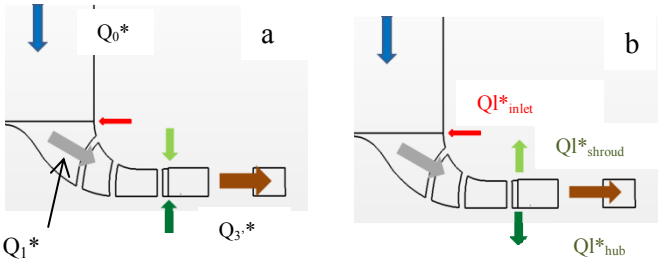

Figure 10. Fluid leakage results

Fluid leakages are calculated for the three different locations (impeller inlet, impeller outlet at the hub and shroud sides). Resulting leakage rates are presented in the Figure 8. Fluid leakages have got a positive value when there is an incoming rate inside the domain. It can be observed, for the inlet gap, that the fluid leakage's rate is always positive. For hub and shroud side leakages, the amount of leakage flow rate depends on the overall flow rate in the pump. At low values of Q_1*(<1), a positive leakage between impeller and diffuser was observed (Figure 10 a). At high values Q_1* (>1) the tendency inverses as shown in Figure 10b. These results were also observed in previous study [9].

Figure 9 presents the evolution of the non-dimensional inlet rates for the domain, the impeller and the diffuser depending on flow rates at the inlet of the domain. These curves show the importance of fluid leakages at low flow rates.

These calculations show the influence of fluid leakages on global performances, especially at the lower flowrates. Global results of static theoretical head pump are in very good agreement between the experimental results and the unsteady calculation results when fluid leakages are taken into account, as it can be seen in Figure 11. The relative differences between numerical calculations without leakages and experimental results are about 10%. The same differences between numerical calculations with leakages and experimental results are lower than 1.3%, considering that the measurement incertitude is greater than this value.

Numerical results obtained when leakages are taken into account show smaller static and total pressure head coefficient compared to those obtained without leakages. This leads to a decrease of impeller efficiency at very low flowrate due to a significant increase of the impeller torque.

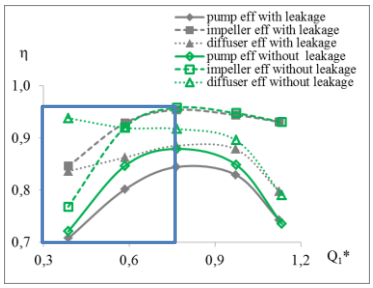

Figure 11. Efficiencies

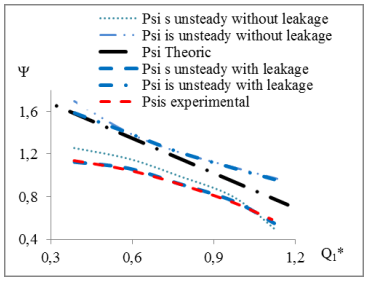

Figure 12. Global performance

Consequently, the pump efficiency due to fluid leakages is lower than those without fluid leakages (Figure 11). The evolution of the diffuser efficiency is quite the same, whatever the leakages are taken into account or not. This is due to the fact that the diffuser is not well adapted at high flowrate. The diffuser design flow rate is close to the value of Q_1*=0.766 as it can be observed.

The global results show a very good agreement between experimental and numerical results with leakage as can be seen in Figure 12.

4.2. Local results

4.2.1 Pressure recovery in the vane diffuser

A temporal mean value of static pressure has been calculated for each radius inside the diffuser from the numerical results. These mean values are compared with the three-holes probe's results. Non-dimensional static pressure levels inside the diffuser in the plane of the probe's positions are drawn in Figure 13 for the three flowrates Q_1*=0.386, Q_1*=0.584 and Q_1*=0.766 respectively for experiments using the three-holes probe (a), for numerical case with leakages (b) and for numerical results without leakages (c). This Figure shows that the results obtained without leakage give bad results compared with experimental ones.

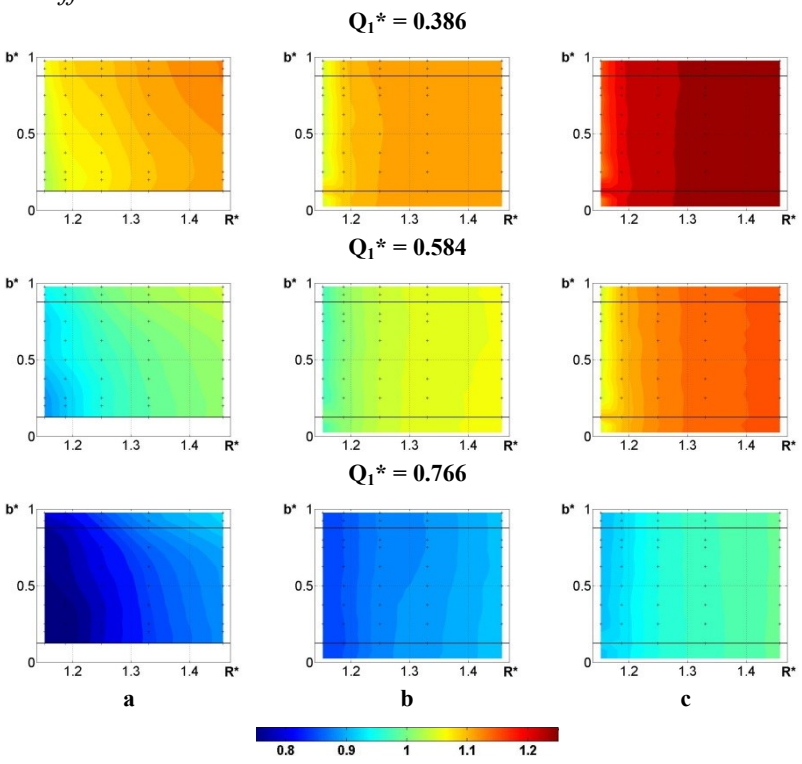

Figure 13. Ψ_S Non dimensional static pressure head inside the diffuser in the plane of the probe's positions

The relative differences are about 10% quite the same as those obtained for overall performances. It can also be observed in this Figure that the evolution of the static pressure, obtained by the numerical calculation with leakage, is quite independent along b*, the value of which is also equal to the experimental results measured near the shroud. In order to show that Ψ_{dS} is quite independent along b* inside the diffuser, the evolution of Ψ_S has been registered for each flowrate Q_1*, for five distances from hub b* (0.125, 0.25, 0.5, 0.75, 0.875) and for the different impeller angular positions relative to the diffuser vanes. This independence is confirmed in the blade to blade channel in diffuser as can be

seen in Figure 14 which is an example of this kind of results. But it can also be observed that, just at the inlet section of the diffuser and up to the diffuser throat, the evolution of pressure depends on b*. The evolution of the pressure at the inlet of the diffuser seems to drive the evolution of leakages at the hub and the shroud which is, in the present study, not constant as modelled in previous studies [5 to 8]. The present calculations show that the leakages are dependant of angular position and impeller's rotating blade to diffuser's blade interaction as can be seen in Figure 15.

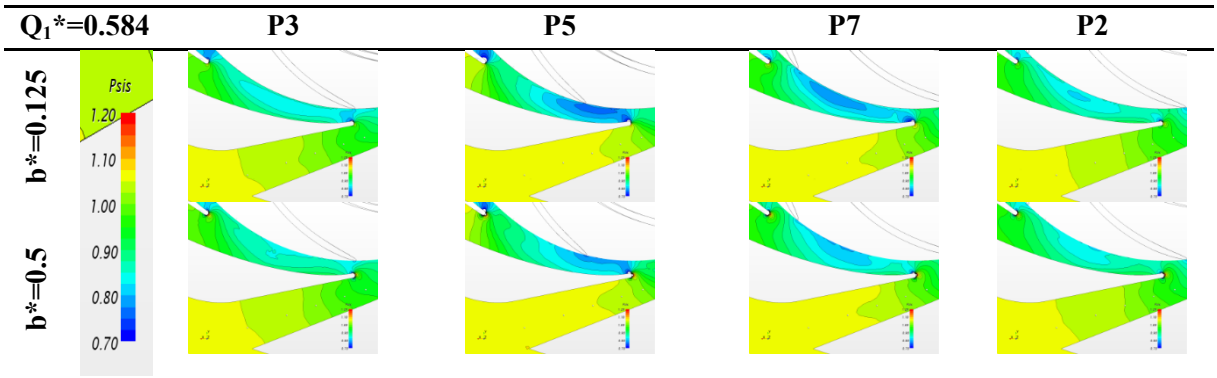

Figure 14. Non-dimensional static pressure inside diffuser

The pressure recovery evolution (Ψ_{ds}) along the diffuser is given in Figure 16. The pressure at the inlet section of the diffuser (which is also the interface between impeller's outlet and diffuser's inlet (R*=1)) can't be measured. In paragraph 4.1, it has been shown that the numerical model with leakages is in good agreement with experimental results for the overall performances. So the static pressure results issued from numerical results obtained with leakage are taken as static pressure values at the inlet section of the diffuser.

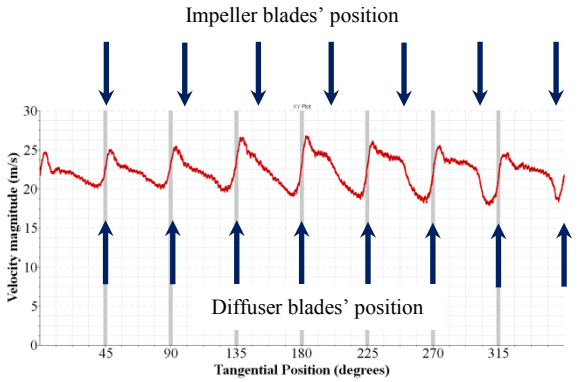

Figure 15. Velocity magnitude of fluid leakages at shroud side in the middle radius of leakages (position P2, radius 257.5 mm, Q_1*=0.386)

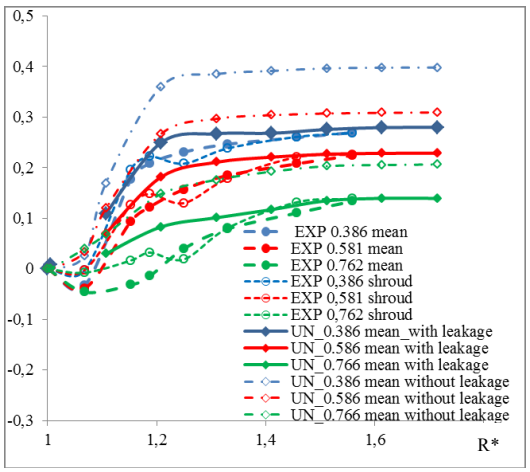

Figure 16. Ψ_{ds} pressure recovery inside the vane diffuser depending on non-dimensional radius R*

Two sets of results can be drawn for the pressure recovery inside the diffuser obtained from the probe measurements. The first one, named "EXP xx mean" represents the arithmetic mean static pressure value between the hub and the shroud (b*=0.975). The second one, named "EXP xx shroud" is calculated with the value of static pressure measured only on the shroud side. These results are compared to mass flow averaged values of pressure in the two calculations cases, with and without leakages. It is obvious that the numerical results obtained without leakages are far away from the experimental ones. On the contrary, the numerical results obtained with leakages give results in good

agreement with experimental results "EXP xx shroud" considering that the three holes probe's method is an intrusive method.

4.2.2 Velocity fields

Now let us compare the velocity fields. 0nly radial velocities (Figure 17) and flow angles (Figure 18) are presented in this paper for four cases: three-holes probe (a), calculation with leakages (b), calculation without leakages (c), PIV measurements (d). The PIV measurements were done only for the next values of b*: 0.125, 0.25, 0.5, 0.75 and 0.875. So only comparisons for b* between 0.125 and 0.875 will be discussed.

Let us remember that the three-holes probe is a method that gives averaged velocities. For the PIV measurements, a software developed by our laboratory was used for the images treatment. The obtained results were then checked and cleared by the same software. Then the data, obtained with the two cameras, were elaborated with a dedicated post processing technique to build a single domain and to calculate fluid-dynamic quantities in the analysis zone (velocity components, flow angles and turbulent rates). In the present study mean values of quantities were calculated between the seven positions Pi. The unsteady calculations give unsteady results which are averaged during a complete rotation of the impeller.

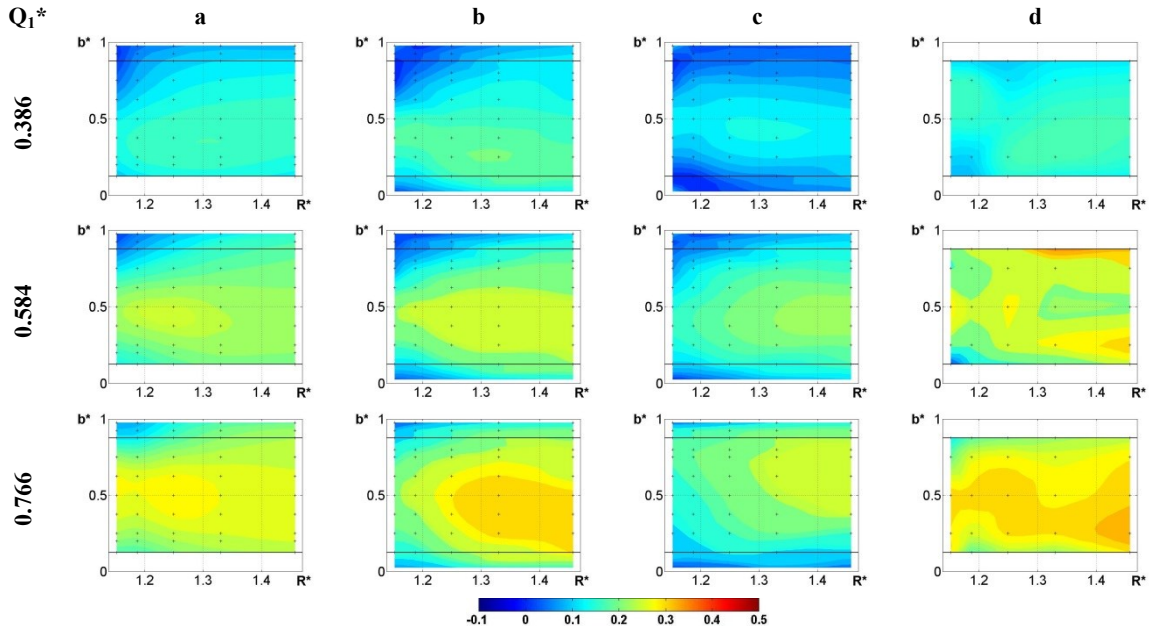

Figure 17. Non-dimensional radial velocity along the diffuser

The examination of experimental results in Figures 17 and 18 leads to question about the validity of the treatment of results of PIV, especially at the inlet of the diffuser (R*<1.2, 0.125>b*<0.975). Some experimental data inconsistencies have been explained by the presence of two vortexes numerically identified at the diffuser entrance on the blade pressure side near the end-walls for Q_1*=0.43 and Q_1*=0.77 by Cavazzini et al [6] and Wuibaut [4].

As for pressure fields, the velocity field shows the bad agreement of the numerical results without leakages.

At the lower flowrate Q_1*=0.386, it can be observed that the three-holes probe measurement, the PIV measurement and the calculations with leakages are in good agreement considering that the PIV measurement gives velocities with a relative accuracy of about 2.2 % for the lower flow rate [6].

At the flowrates Q_1* =0.584 and Q_1* =0.766, the agreement between numerical calculations and experimental results is not too bad. The values of numerical calculations are comprised between the two experimental results.

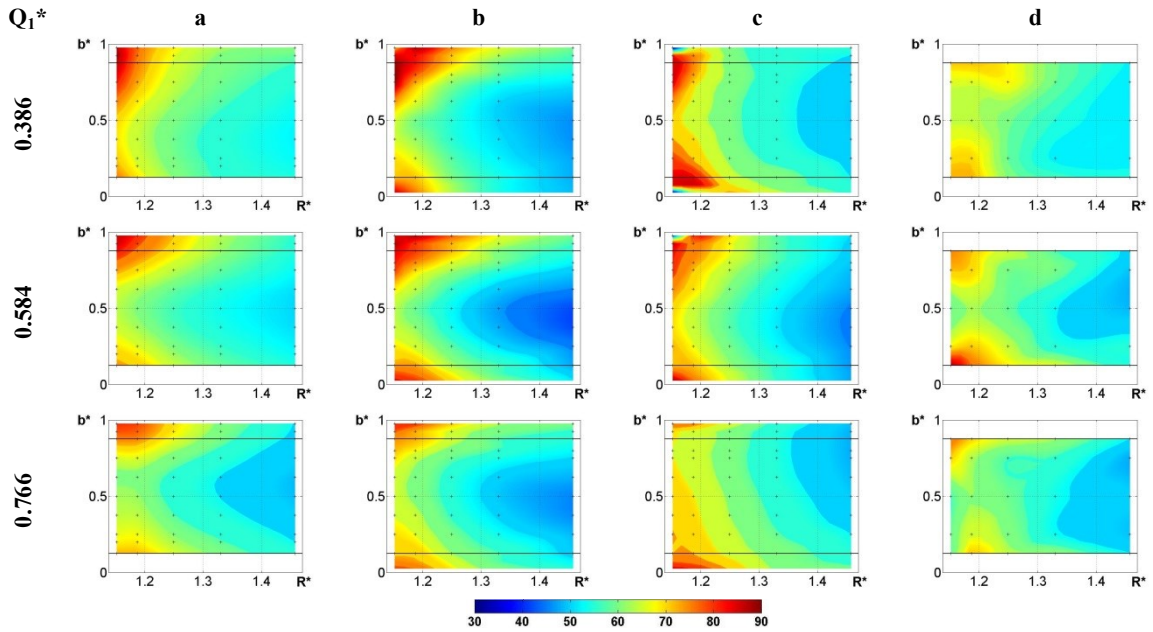

Figure 18. Flow angle α inside the diffuser

5. Conclusion

The SHF pump with vaned diffuser was studied at three low flow rates. Two experimental techniques measurement's results, already used to analyse in detail the flow field in one blade diffuser passage, were compared with those of numerical computations performed by URANS model (SST k-ω turbulence model) with and without leakages modelled.

The comparisons between numerical calculations with leakages modelled and experimental results highlighted few differences. The global and the local results were discussed. The leakage flow rates greatly affect the global performance and the flow inside the diffuser. These leakages' flows are influenced by the impeller-diffuser interaction effects. At low flow rates, the leakage flow rate entered into the gaps and interacted with the impeller blade wakes creating vortexes on the pressure side of the diffuser blade that probably affect the velocity PIV measurements.

The experimental results were in good agreement with the numerical data with leakages modelled.

In the present studies, the comparisons were done with mean values. It will be interesting to go on with deeper analysis on instantaneous fields.

Nomenclature

b	Distance from hub [m]
b^*	Non-dimensional distance from hub (=b/B)
B	Diffuser Blade height [m]
C	Impeller torque [mN]
dp_s	Static pressure difference [Pa] $(=p_s-p_{s1})$
dp_t	Total pressure difference [Pa] $(=p_t-p_{t1})$
dp_{ti}	Impeller total pressure difference [Pa] $(=p_{t2}-p_{t1})$
dp_{tp}	Pump total pressure difference [Pa] $(=p_{t4}-p_{t1})$
N	Rotational speed [rpm]
p_s	Static pressure [Pa]
p_t	Total pressure [Pa]
Q_1^*	Non-dimensional volume flowrate at impeller's inlet$(=Q/Q_i)$
Q_d	Diffuser design flowrate [m^3/s]
Q_i	Impeller design flowrate [m^3/s]
Q_l^*	non-dimensional flowrates of fluid leakage $(=Q_l/Q_i)$
R	Radius [m]
η_d	Diffuser efficiency $(=\eta_p/\eta_i)$
α	Absolute velocity angle relative to radial direction $(=Arctg(Vu/Vr))$
ρ	Air density [kg/m^3]
Ω	Angular Velocity [rad/s] $(=\pi N/30)$
Ψ_i	Non-dimensional isentropic head $(=C\Omega/(\rho Q U_2^2/2))$
Ψ_s	Non-dimensional static pump head $(=dp_s/(\rho U_2^2/2))$
Ψ_{ds}	Non-dimensional pressure recovery $(=(p_s-p_{s2})/(\rho U_2^2/2))$
Ψ_{tp}	Non-dimensional total impeller head $(=dp_{ti}/(\rho U_2^2/2))$
Ψ_{ti}	Non-dimensional total pump head $(=dp_{tp}/(\rho U_2^2/2))$

Index

d	Diffuser

R^*	Non-dimensional radius $(=R/R_2)$	i	Impeller
V_r	Radial velocity [m/s]	p	Pump
V_r^*	Non-dimensional radial velocity $(=V_r/U_2)$	0	Domain inlet
V_u	Tangential velocity [m/s]	1	Impeller inlet
V_u^*	Non-dimensional tangential velocity $(=V_u/U_2)$	2	Blade's Impeller outlet
U_2	Frame velocity at blade's impeller outlet [m/s] $(=\Omega*R_2)$	$2'$	Impeller outlet (hub and shroud)
		$3'$	Diffuser inlet (hub and shroud)
Z_d	Number of diffuser blades	3	Blade's diffuser inlet
Z_i	Number of impeller blades	4	Blade's diffuser outlet
η_p	Pump efficiency $(=\Psi_{tp}/\Psi_t)$	$4'$	Diffuser outlet (hub and shroud)
η_i	Impeller efficiency $(=\Psi_{ti}/\Psi_t)$		

References

[1] Runstadler PW, Dolan FX, Dean RC 1975 *Diffuser Data Book: Diffuser Data and Interpretation* Creare Inc
[2] Japikse D 1996 *Centrifugal compressor design and performance* Wilder VT: Concepts ETI Inc
[3] Wuibaut G, Dupont P, Caignaert G, Stanislas M 2000 Experimental analysis of velocities in the outlet part of a radial flow pump impeller and the vaneless diffuser using particle image velocimetry, *Proceedings of the XX IAHR Symposium* (Charlotte, USA) 6-9 August **paper GU-03**
[4] Wuibaut G 2001 Etude par vélocimétrie par images de particules des interactions roue-diffuseur dans une pompe centrifuge PhD thesis (Lille, France)
[5] Cavazzini G 2006 Experimental and numerical investigation of the rotor-stator interaction in radial turbomachines Ph.D. thesis (Padova, Italy)
[6] Cavazzini G, Pavesi G, Ardizzon G, Dupont P, Coudert S, Caignaert G, Bois G 2009 Analysis of the rotor-stator interaction in a radial flow pump *La Houille Blanche* **5** pp141-151
[7] Cavazzini G, Dupont P, Pavesi G, Dazin A, Bois G, Atif A, Cherdieu P 2011 Analysis of unsteady flow velocity fields inside the impeller of a radial flow pump : PIV measurements and numerical calculation comparisons *Proc. of ASME-JSME-HSME Joint Fluids Engineering Conference* (Hamamatsu, Japan)
[8] Si Q, Dupont P, Bayeul-Lainé AC, Dazin A, Roussette O, Yuan S 2015 An experimental study of the flow field inside the diffuser passage of a laboratory centrifugal pump *ASME Journal of Fluids Engineering* **137** pp1-12
[9] Bayeul-Lainé AC, Dupont P, Cavazzini G, Cherdieu P, Dazin A, Bois G, Roussette O 2013 Numerical and experimental investigations in a vaned diffuser of SHF impeller : fluid leakage effect *21 èmeCongrèsFrançais de Mécanique* (Bordeaux)
[10] Bayeul-Lainé AC, Dupont P , Miccoli L, Cavazzini G, Dazin A, Pavesi G, Bois G 2014 Fluid leakage effect on analysis of a vaned diffuser of SHF pump *15th International Symposium on Transport Phenomena and Dynamics of Rotating Machinery ISROMAC-15* (Honolulu, USA)
[11] Bayeul-Lainé AC, Dupont P, Cavazzini G, Pavesi G, Dazin A, Cherdieu P, Bois G Roussette O 2015 Comparisons RANS and URANS numerical results with experiments in a vaned diffuser of a centrifugal pump *La Houille Blanche* pp108-116
[12] Dupont P, Bayeul-Lainé AC, Dazin A, Bois G, Roussette O, Si Q 2015 Leakage Flow Influence on SHF pump model performances *International Journal of Fluid Machinery and Systems* **8 (4)** pp274-282
[13] Morel P 1993 *Ecoulements décollés dans une pompe de roue centriguge* PhD Thesis (Lille, France)
[14] Menter FR, Kuntz M 2002 Adaptation of Eddy Viscosity Turbulence Models to Unsteady Separated Flows Behind Vehicles *The Aerodynamics of Heavy Vehicles: Trucks, Buses and Trains* Springer (Berlin) pp 339-352
[15] Cherdieu P 2014 *Contrôle du décollement dans un diffuseur aubé de turbomachine centrifuge* PhD thesis (Lille, France)